J Incl Phenom Macrocycl Chem (2012) 73:387–396
DOI 10.1007/s10847-011-0076-6

ORIGINAL ARTICLE

Surfactant-assisted intercalation of crystal violet in layered γ-zirconium phosphate. Dye uptake from aqueous solutions

**Hussein M. H. Alhendawi · Ernesto Brunet ·
Elena Rodríguez Payán · Olga Juanes ·
Juan Carlos Rodríguez Ubis · Muhammad Al-Asqalany**

Received: 30 June 2011 / Accepted: 24 October 2011 / Published online: 17 November 2011

Abstract Batch intercalation experiments have carried out using γ-zirconium phosphate (γ-ZrP) and one of its cationic surfactant forms (γ-ZrP/SUR$^+$) for removing crystal violet from aqueous solutions. The intercalation reactions have conducted along two different intervals of time (24 and 48 h). The intercalation process has followed up by X-ray diffractometry (XRD), UV–Visible and FT-IR spectrophotometries. Regarding γ-ZrP, XRD patterns show that obtained phases are impure, even after 48 h of the reaction time at a maximum dye loading of 18%. On the other side, γ-ZrP/SUR$^+$ gives an impure phase after 24 h while a pure one (2.47 nm) is obtained after 48 h at a maximum dye loading of 19%. In both cases, the observed dye loading values are approximately equal to the one calculated by molecular modeling (ca. 20%). The used analysis approaches prove that dye uptake capacity is a function of the reaction time and inclination angle of the dye molecules inside the solid matrices, where the highest dye uptakes are observed with γ-ZrP and γ-ZrP/SUR$^+$ after 48 h of the reaction time. This time (48 h) is long enough for the dye molecules to be sufficiently accumulated inside the interlayer regions, in such situation dye molecules are forced to stand up perpendicular to the inorganic layers. With respect to intercalation properties, the difference between γ-ZrP and γ-ZrP/SUR$^+$ could be referred to the difference between their gallery heights (1.22 and 3.00 nm, respectively). The pre-intercalation of γ-ZrP with the surfactant molecules assists the inclusion and intercalation of the huge dye molecules into the interlayer region.

Keywords γ-zirconium phosphate · Cationic surfactant · Intercalation · Dye uptake · Crystal violet

Introduction

Many industries such as textile, paper, plastic, leather tanning, ceramics, cosmetics, food, glass, paints, soap, wax biomedicine etc., use dyes extensively in different operations. Moreover, dyes have significant importance in the field of microbiology. They are used to make the micro-organisms distinctly visible and/or differentiate them. For example, Crystal violet *(N,N,N′,N″,N″,N″*-hexamethylpararosalinine), triphenylmethane dye, has been used extensively in textile dyeing and dye-stuff manufacturing industries, in human and veterinary medicines as a biological strain and in paper, leather, food and cosmetic processing industries [1, 2]. This dye has been categorized as a recalcitrant molecule indicating that, it is poorly metabolized by microbes and therefore, is persistent in environment for longer period when discharged [3].

The dyestuff industries discharge variety of pollutants in different processes. Purification of water and air resources that contain even traces of dyes is an important technological challenge and has attracted wide attention. Removal of dyes by conventional waste treatment methods is difficult since these are stable to light and oxidizing agents and

---

H. M. H. Alhendawi (✉)
Department of Chemistry, Faculty of Science,
Al-Azhar University of Gaza, 1277 Gaza, Palestine
e-mail: hussein.alhendawi@yahoo.com

E. Brunet · E. R. Payán · O. Juanes · J. C. R. Ubis
Departamento de Química Orgánica, Facultad de Ciencias
C-I-602, Universidad Autónoma de Madrid, 28049 Madrid,
Spain

Present Address:
M. Al-Asqalany
Department of Health Professions, University Collage
of Applied Sciences, 1415 Gaza, Palestine

are resistant to aerobic digestion. Therefore, creation and chemical engineering of new kinds of porous materials able to efficiently entrap dyes is thus quite desirable.

Various kinds of treatments technologies such as adsorption, chemical flocculation, chemical oxidation, froth flotation, ultra filtration and biological treatment technologies have been employed. The worth mentioning is that, layered zirconium phosphates (ZrP) can be considered as promising materials for removing dyes from aqueous solutions.

Basically, α- and γ-ZrP phases share the same elemental composition but slightly different empirical formulae [$Zr(HPO_4)_2 \cdot nH_2O$ for α-type and $Zr(PO_4)(H_2PO_4) \cdot nH_2O$ for γ-type]. Their structure is significantly different (Fig. 1).

In addition, zirconium phosphate is a layered salt (Fig. 1) whose intercalation properties has been extensively investigated due to its interesting fundamental aspects and its possible applications as well [4–6], including ion exchange, high-temperature stable organic–inorganic composites, ion conduction, catalysis, etc. Yet, there are scant publications concerning the use of ZrP for the entrapment of dyes from wastewater or other sources [7–11]. Two methodologies were applied in this field: (1) the use of ZrP as photocatalyst support in the photocatalytic degradation of dyes [5]; (2) sorption and/or intercalation of dyes in α- and γ-type of ZrP [8–11].

In the most recent paper [11], we have used γ-ZrP and surfactant-treated γ-ZrP for the first time in removal of dyes from aqueous solutions. These two layered materials revealed efficiently in removal of malachite green ($[C_6H_5C(C_6H_4N(CH_3)_2)_2]Cl$). The dye uptake capacities of them were 245.45 and 286.67 mg g^{-1}, respectively. Therefore, further investigations in this field are valuable and highly recommended.

The current study investigates the intercalation of crystal violet (CV; Fig. 2) in the interlayer regions of γ-ZrP with and without the intermediation of the cationic surfactant Praepagen HY.

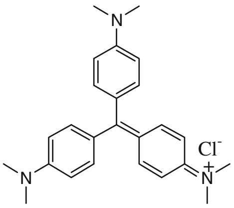

Fig. 2 Structure of the crystal violet (CV)

The intercalation of γ-ZrP with surfactants causes an increase of the *d* spacing with respect to that of the precursor [11, 12] which could facilitate the inclusion of huge molecules like dyes into the interlayer region. The elemental and thermogravimetric analyses, UV–Visible and FT-IR spectrophotometries and the seen interlayer distances using X-ray diffractometry (XRD) are mainly used for observing the dye uptakes.

Theoretically, dye uptakes are discussed in terms of the constant free area available around each surface phosphate, the molecular dimensions of the dye, and the mode of arrangement of the dye molecules inside the solid matrices.

Experimental

All chemicals and reagents used were analytical grade. All of them except Praepagen HY surfactant (Clariant) were purchased from Aldrich Co., and used as supplied. γ-ZrP was prepared by the HF method (interlayer distance 1.22 nm; cf. Figure 1) [13].

Intercalation procedures

Intercalation of HY surfactant in γ-ZP

Solid γ-ZrP (5.00 g, 15.7 mmol) was suspended in 500 mL of a 0.1 M aqueous solution of methyl ammonium chloride. To the suspension a 0.1 M solution of methylamine was slowly added until pH = 9. The solid was then centrifuged and washed with distilled water (3 × 500 mL).

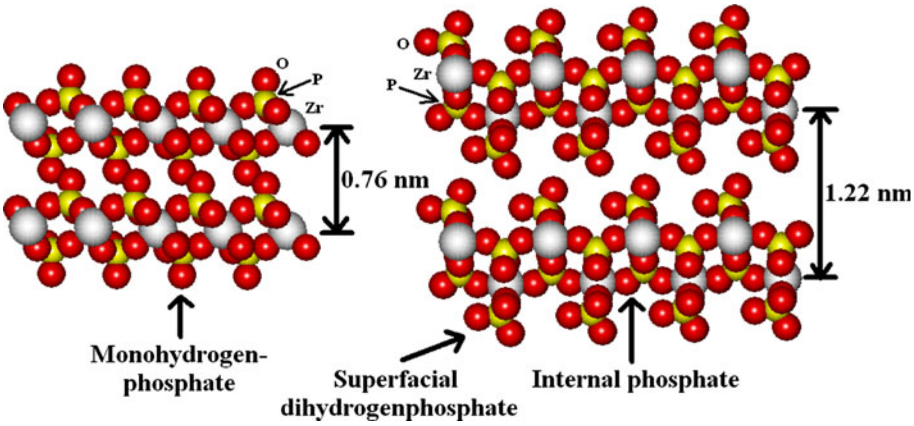

Fig. 1 Space-filling models of two consecutive layers formed by octahedral–tetrahedra building-block combination: **a** α-ZrP (*left*) **b** γ-ZrP (*right*). Hydrogen has been omitted for sake of clarity

The solid was suspended in 783 mL of a 0.1 M solution of HY surfactant (1:5 γ-ZrP:HY mole ratio). The mixture was stirred at room temperature for 48 h and the solid was again centrifuged and washed with distilled water (3 × 500 mL). The solid was dried in the oven at 100 °C for 24 h and conditioned at least three days in a desiccator containing saturated solution of $BaCl_2$ yielding 5 g of a pale yellow solid denoted as γ-ZrPHY.

Intercalation of CV in γ-ZP

Solid γ-ZrP (500 mg, 1.57 mmol) was suspended in 523.3 mL of a 1.5×10^{-2} M solution of the dye in water, the mole ratio of γ-ZrP to dye results 1:5. The mixture was stirred at room temperature for 24–48 h. The solid was centrifuged, washed with water, centrifuged until the supernatant solution gets colourless (25 × 60 mL), dried in the oven at 100 °C for 24 h and finally conditioned at least three days in a desiccator containing saturated solution of $BaCl_2$. Two solids were prepared by this procedure: one separated after 24 h (500 mg) and denoted as CV1 and the other separated after 48 h and denoted as CV2 (480 mg).

Intercalation of CV in surfactant-treated γ-ZP (γ-ZPHY)

Solid γ-ZrPHY (500 mg, 1.00 mmol) was suspended in 333.3 mL of a 1.5×10^{-2} M solution of the dye in water, the mole ratio of γ-ZrPHY to dye results 1:5. The mixture was stirred at room temperature for 24–48 h. The solid was centrifuged, washed with water, centrifuged until the supernatant solution gets colourless (20 × 60 mL), dried in the oven at 100 °C for 24 h and finally conditioned at least three days in a desiccator containing saturated solution of $BaCl_2$. Two solids were prepared by this procedure: one separated after 24 h and denoted as CV3 (500 mg) and the other one separated after 48 h and denoted as CV4 (450 mg).

Characterization

XRD patterns were recorded at room temperature on either Phillips PW1710 or Siemens D-5000 diffractometers with Cu Kα radiation ($\lambda = 0.154$ nm) and Ni filter at 40 kV, 30 mA, a scanning rate of 5° $\min^{-1}$, and a 2θ angle ranging from 3° to 70°. The UV–Vis spectra were obtained on a UV-1601 spectrophotometer (SHIMADZU-JAPAN). Infrared spectra for the materials were recorded on a FTIR-8201PC spectrometer (SHIMADZU-JAPAN) using KBr disk in the range 4,000–400 cm^{-1}. Elemental analyses were performed on a Perkin Elmer II 2400 CHN analyzer. Thermogravimetric analysis was performed on a Mettler-Toledo TGA/STDA 851e apparatus and recorded at 5 °C/min. The TG-DTA curves have been obtained under nitrogen sweeping. Structure modeling was carried out on PC computers using the Hyperchem release 7 and the semiempirical method AM1.

Results and discussion

Intercalation of CV in γ-ZrP

Initially, it is well known that intercalation chemistry of γ-ZrP is dominated by the presence in the interlayer region of Brønsted acid groups. Species with sites able to accept protons are the preferred guests. The insertion of the guest occurs concomitantly in each interlayer region from the border of the crystallites toward the center with an advancing phase boundary, and it may happen that the intercalation of a single quest leads to the formation of various intercalated phases that differ from each other in composition and interlayer distance [14].

The intercalation process of CV in the pristine γ-ZrP is supposed to be accompanied by an acid–base reaction between the amino groups of the dye and the superficial $O_2P(OH)_2$ groups of the inorganic layers. As a result of this reaction, the dye monovalent cations (CV^+) are expected to be converted to doubly protonated ones ($CVHH^{3+}$) inside the solid matrices. Therefore, the electrostatic ionic interaction is considerably expected to be the main type among supramolecular host–guest interactions.

Actually, all of intercalation reactions in this research are conducting in aqueous media. CV is apolar and lipophilic molecule while the layers of γ-ZrP are highly polar. Consequently, the absorption of hydrated dye molecules should be more efficient than that of non-hydrated.

In practice, two intercalation compounds are obtained as a result of intercalation of the CV dye in γ-ZrP, denoting the products as CV1 and CV2. These products are separated after 24 and 48 h, respectively. CV1 gives a C, H, N, Cl % content of 12.70, 2.73, 1.78, 1.44 (calculated: 12.68, 2.74, 1.78, 1.48), respectively, corresponding to the formula $ZrPO_4(H_2PO_4)(C_{25}H_{30}N_3Cl)_{0.16}\cdot 1.75H_2O$. On its part, CV2 gives a C, H, N, Cl % content of 23.55, 3.51, 3.30, 2.85 (calculated: 23.57, 3.54, 3.30, 2.75), respectively, corresponding to the formula $ZrPO_4(H_2PO_4)(C_{25}H_{30}N_3Cl)_{0.36}\cdot 1.65H_2O$.

As remarkable comments on the mentioned above analysis, the existence of one mole of chloride ions per mole of dye molecules in the chemical formulae of the materials CV1 and CV2 emphasizes the presence of acid–base reaction between CV and γ-ZrP.

The XRD patterns of both materials (Fig. 3) show that they are impure phases. Regarding CV1, two peaks were observed corresponding to distances of 1.18 and 1.71 nm. While CV2 shows two peaks equivalent to separations of 1.22 and 2.45 nm.

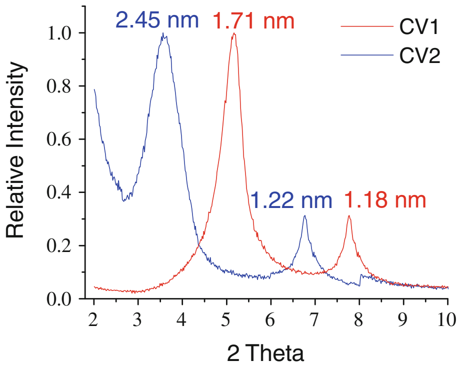

Fig. 3 X-ray powder diffraction patterns of CV1 and CV2

Figure 4 shows the calculated structures (semiempirical method AM1) for the predicted most stable conformations of CV^+ and $CVHH^{3+}$. The estimated molecular dimensions are also indicated. The thickness of one γ-ZrP layer is 0.9 nm. Therefore, the measured distance for CV1 (1.71 nm) leaves separation of ca. 0.81 nm for intercalate. Although this interlayer separation is not large enough for CV molecule to have a position perpendicular to the inorganic layers, it permits an inclination angle much greater than zero. Figure 5a shows the calculated structure in which $CVHH^{3+}$ trivalent cations are arranged parallel to the inorganic layers (zero angle of inclination). Regarding the measured distance for CV2 (2.45 nm), it leaves a separation of ca. 1.55 nm for intercalate which is large enough for the CV molecules (length = 1.36 nm) to be perpendicularly positioned inside the interlayer gallery.

Figure 5b reveals a plausible arrangement of $CVHH^{3+}$ cations within γ-ZrP which is compatible with the measured interlayer distance in CV2 where CV cations are arranged perpendicular to the inorganic layers.

In order to estimate the maximum ion-exchange capacity of γ-ZrP, let's consider a fraction of γ-ZrP formed by two layers of 100 Zr atoms apiece. Each of the four surfaces will bear 50 phosphates and the interlayer region will be thus populated by 50 + 50 opposed phosphates. The available room around every surface phosphate is around 0.36 nm^2 (Fig. 6) [12]. Thus each face of the taken fraction of γ-ZrP has a total area of $0.36 \times 50 = 18$ nm^2. For parallel arrangement, the surface covered by one CV molecule is ca. 1.81 nm^2 however it is ca. 0.46 nm^2 for perpendicular arrangement. Accordingly, surface coverage values of parallel and perpendicular arrangements correspond to ca. 10 and 36–38 molecules, respectively, to be placed within the taken model of two layers of 100 Zr atoms apiece.

With respect to the recent estimation and calculations, it could be concluded that the dye uptake capacity is fully affected by the mode in which CV molecules are arranged inside the interlayer gallery.

According to the performed chemical analyses, CV1 and CV2 materials have 16 CV and 36 CV molecules per formula (vide supra), respectively. This mostly leads to the existence of acute and vertical angles for CV molecules with respect to the inorganic layers in CV1 and CV2 (Fig. 5), respectively.

The calculated chemical formulae of CV1 and CV2 are confirmed by differential thermal analysis (DTA; Fig. 7).

The DTA curves show that there is weight loss between 25 and 150 °C caused by the hydration water (8.33 and 6.49, respectively). CV1 and CV2 show similar thermal behavior between 350 and 650 °C where the dye decomposes. This decomposition corresponds to weight losses of 17.32 and 32.22%, respectively. The later percentages are compatible with the calculated amount of the dye in the formulae of CV1 and CV2 (17.21 and 32.00%, respectively).

The UV–Vis. spectra of CV1 and CV2 are recorded in suspension (Fig. 8). The suspensions are prepared by sonication of equal amounts of the solid samples (8 mg) in 10 mL of water for 10 min. Crystal violet exhibits a strong absorption band at 590 nm ($\pi \rightarrow \pi^*$ transition; Fig. 8), which is a characteristic band for crystal violet dye. This band is strongly red-shifted by 42 nm for CV1 and CV2 (Fig. 8). In addition, the UV–Vis is spectra of the two materials show a new band at 440 nm which is referred to doubly protonated CV^+. The comments regarding the red-shift and new band are consistent with publications found concerning CV dye [15] and α-ZrP/CV composite [9].

Fig. 4 Predicted most stable conformation of crystal violet (Hyperchem, AM1): **a** CV^+ **b** $CVHH^{3+}$

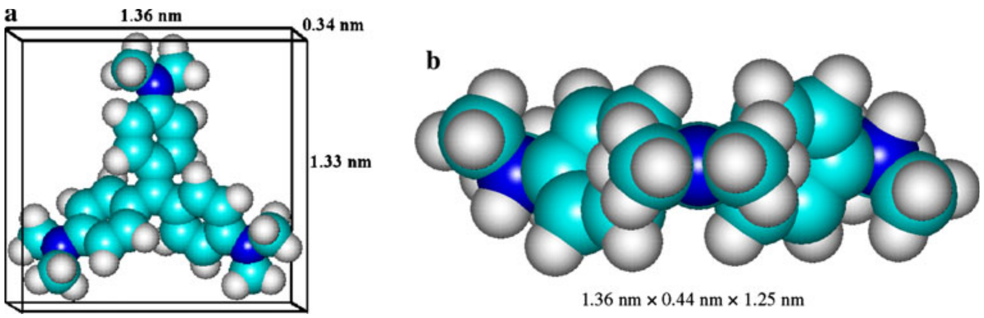

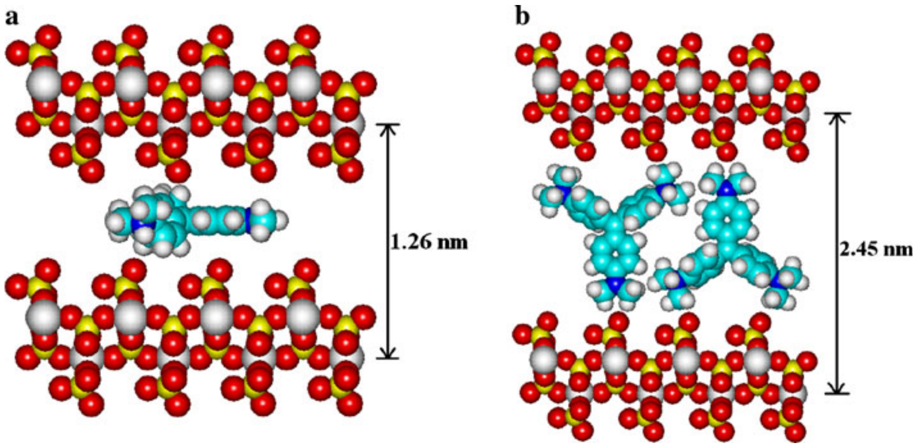

Fig. 5 Calculated structures of $CVHH^{3+}/\gamma$-ZrP composites: **a** CV cations are arranged parallel to the inorganic layers (zero angle of inclination). The estimated interlayer distance is indicated. **b** Possible arrangement of CV cations intercalated in γ-ZrP complying with the observed interlayer distance of CV2

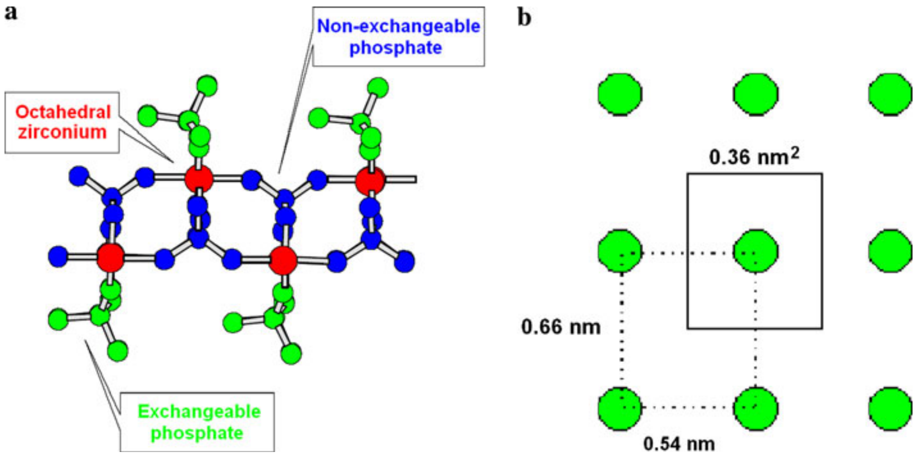

Fig. 6 Schematic representation of the grid formed by superficial phosphates in a face of one layer of γ-ZrP. The distances between adjacent phosphates and available area are indicated

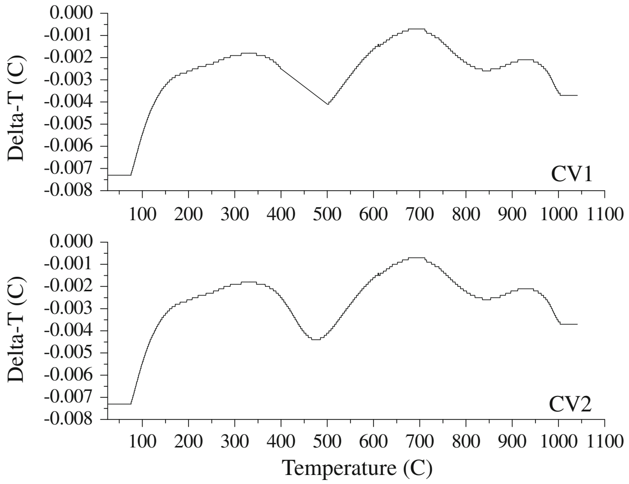

Fig. 7 DTA curves of CV1 and CV2

$CV^{+} + H^{+} \rightleftharpoons CVH^{2+} + H^{+} \rightleftharpoons CVHH^{3+}$.

As a reasonable clarification for the recent comments, the dye in solution is monovalent cation (CV^{+}) while in CV1 and CV2 is trivalent. So the dye should have different conjugated systems.

This explanation is in accordance with the proposed acid–base reactions between CV and γ-ZrP. When CV molecule reacts with γ-ZrP, it abstracts two protons from its $O_2P(OH)_2$ groups, and it is converted from monovalent cation (CV^{+}) to trivalent one ($CVHH^{3+}$).

As a result from the measurement of absorbance values, CV2 has higher absorbance (1.31) than CV1 (0.66), therefore CV2 dye content is higher than that one in CV1. This result seems to be in accordance with the calculated chemical formulae of CV1 and CV2.

Figure 9 shows the FT-IR spectra of the free CV dye, γ-ZrP, CV1 and CV2. FT-IR spectrum of free CV dye revealed strong peaks at 1,173 cm^{-1} (H_3C–N stretch) and 1,364 cm^{-1} (aromatic tertiary amine, CN stretch) and a medium one at 1,470 cm^{-1} and a strong one at 1585 cm^{-1} (aromatic rings, CC stretch).

Regarding FT-IR spectrum of γ-ZrP (Fig. 9), it shows its typical characteristic peaks [16]: the peak at 550 cm^{-1} corresponds to δ (PO_4), while the peak at 900 cm^{-1} characterizes a strong H-bond. The band at 1,620 cm^{-1} belongs to the bending vibrations of water molecules. The peak at 1,100 cm^{-1} is attributed to the (PO_4) stretching vibrations, while the broad band in the region 3,500–3,000 cm^{-1}

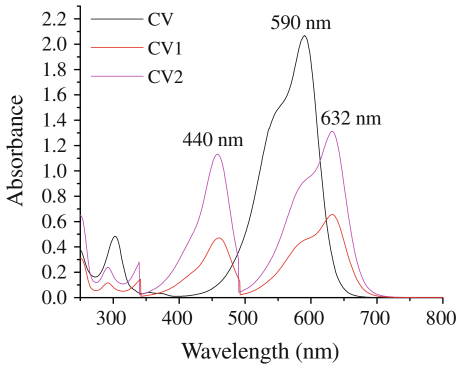

Fig. 8 UV–Vis spectra of CV aqueous solution (8.6 × 10^{-4} M) and CV1 and CV2 (suspension of 8 mg of the solid in 10 mL of water)

corresponds to symmetric and asymmetric stretching vibrations of water molecules and OH groups.

In case of CV1 and CV2, the FT-IR spectra are mostly composites of those of γ-ZrP and free dye, except for the absorption bands around the region 1,600–1,400 cm^{-1}, where these bands assigned to the CC stretching vibrations of the aromatic rings, appear in the spectrum of free CV dye. It can be concluded that, upon protonation these bands shift to higher frequencies, as in the case of porphyrins [17] and α-diimines [18]. Thus, the free CV dye has strong absorption at 1,585, 1,470, 1,364 and 1,173 cm^{-1}, whereas these bands almost disappeared in the intercalates. Instead, the bands around 1,620 cm^{-1} are found to be strengthened. As the host γ-ZrP has a band at 1,620 cm^{-1} due to the bending vibration of water; we consider that the strengthened absorptions are due to the superposition of absorption of water and the protonated CV dye. Since CV2 has higher dye content than that one in CV1, this band (at 1,620 cm^{-1}) is more intense in FT-IR spectrum of CV2. Accordingly, the intensity of the recent band in CV1 and CV2 spectra is mostly compatible with the calculated chemical formulae of those materials.

Intercalation of CV in surfactant-treated γ-ZrP (γ-ZrPHY)

Although γ-ZrP exhibits a very high dye uptake (18%) towards CV in the direct batch intercalation method used in the current study, impure intercalation phases are obtained even after 48 h of the reaction time.

The presence of impure phases indicates that the huge CV molecules encounter difficulties in the diffusion into the interlayer region. So these molecules are not equally distributed over the internal surfaces of the inorganic layers resulting in the observation of more than one reflection peak in the X-ray patterns of CV1 and CV2 (Fig. 3). In order to overcome the problem of molecules diffusion, an alternative indirect strategy is followed based on the fact that the previously exchanged organic [11, 19, 20] or inorganic [21] cations can be replaced by another ones.

In practice this strategy is already tested and implemented successfully within one of our recent papers which is titled with “Intercalation of Malachite Green ($[C_6H_5C(C_6H_4N(CH_3)_2)_2]Cl$) in Layered γ-Zirconium Phosphate. Effect of cationic surfactants” [11].

Fig. 9 FT-IR spectra of the free CV dye, γ-ZrP, CV1 and CV2

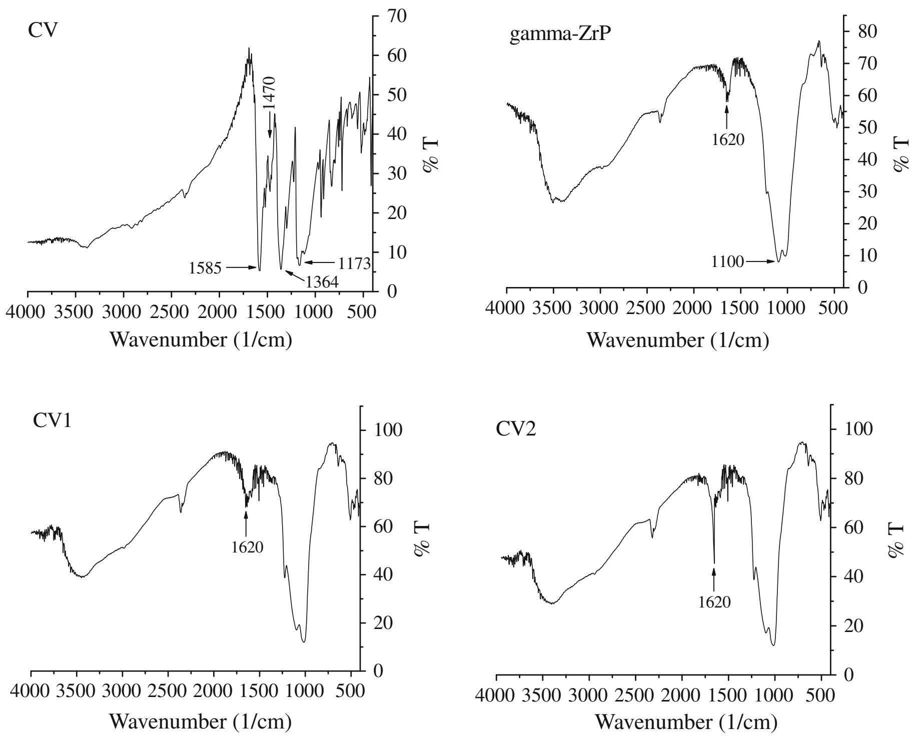

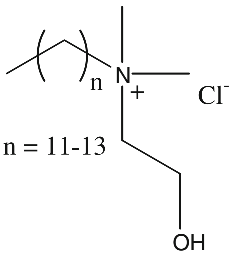

Fig. 10 Alkyl-*N*-ethanol-*N,N*-dimethylammonium chloride (Praepagen HY surfactant)

The intercalation of surfactants in γ-ZrP leads to expanded interlayer separation. Once the kinetic barrier to larger separation has been removed, surfactant molecules can be subsequently exchanged with appropriate quest molecules to generate organized supramolecular assemblies. In order to facilitate the inclusion chemistry of γ-ZrP, its pH was adjusted at 9 by methyl amine then intercalated with a cationic surfactant commonly called Praepagen HY (see "Experimental" section). The IUPAC name of this surfactant is alkyl-N-ethanol-*N,N*-dimethylammonium chloride (alkyl group: C_{12}–C_{14}, Fig. 10).

The chemical formula of γ-ZrP/HY surfactant composite (γ-ZrPHY) was calculated as $ZrPO_4(H_2PO_4)(C_{17}H_{38}NO)_{0.64}(CH_5N)_{0.32}\cdot1.80H_2O$. This surfactant-treated material displays an interlayer spacing of 3.00 nm, as compared to 1.22 nm of the starting material (γ-ZrP) [11].

The reaction between CV and γ-ZrPHY is expected to be a double replacement reaction. In the matter of reaction, the methyammonium cations and the HY cations are expected to be partially replaced by the dye cations (CV^+) where the partial replacement should be mainly attributed to the large molecular size of the dye.

The worth mentioning that, first, the interaction between methyammonium cations ($MeNH_3^+$) and the negatively charged phosphate groups of the host is mainly electrostatic ionic interaction. Second, the double replacement of these recent intercalated cations by surfactant (HY^+) and monovalent unprotonated dye (CV^+) cations means that the ionic interaction stills the most effective and predominant interaction type among various non-covalent supramolecular host–guest interactions such as hydrogen bonding, ion–dipole and dipole–dipole interactions.

Practically, two intercalation compounds are obtained as a result of intercalation of the dye CV in γ-ZrPHY, denoting the products as CV3 and CV4, respectively. These products are separated after 24 and 48 h, respectively. CV3 gives a C, H, N % content of 20.60, 4.00, 2.75 (calculated: 20.46, 4.05, 2.79), respectively, corresponding to the formula $ZrPO_4(H_2PO_4)(C_{25}H_{30}N_3)_{0.18}(C_{17}H_{38}NO)_{0.15}(CH_5N)_{0.15}\cdot1.55H_2O$. On its part, the C, H, N % content of CV4 found: 28.22, 4.35, 4.10 (calculated: 28.27, 4.33, 3.91), respectively, leads to several compatible formulae in which small amounts of HY and methylammonium have to be included [i.e. $ZrPO_4(H_2PO_4)(C_{25}H_{30}N_3)_{0.38}(C_{17}H_{38}NO)_{0.10}(CH_5N)_{0.10}\cdot1.45H_2O$].

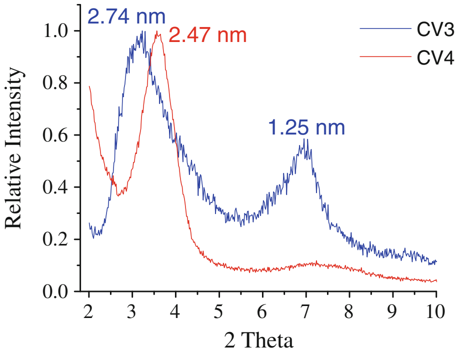

Fig. 11 X-ray powder diffraction patterns of CV3 and CV4

As one of the most important points to be mentioned, the absence of chloride in the chemical formula of CV3 and CV4 emphasizes the double replacement reaction between CV and γ-ZrPHY.

Figure 11 shows the XRD patterns of both materials. As the first part of XRD interpretation, CV3 shows two peaks which are in correspondence with distances of 1.25 and 2.74 nm. Second, CV4 presented only one discernible peak equivalent to a separation of 2.47 nm.

Moreover, CV3 can be considered as an impure intermediate phase between the starting material (γ-ZrPHY) at zero reaction time and the dye intercalated phase separated after 48 h (CV4), in contrast CV4 is almost purer in phase than CV3.

$$\begin{array}{lll} \gamma\text{ - ZrPHY } + \text{ CV } \rightarrow & \text{CV3 } + \text{ CV } \rightarrow & \text{CV4} \\ 3.00\text{ nm} & (1.25\text{ nm}, 2.74\text{ nm}) & 2.47\text{ nm} \\ t = 0 & t = 24\text{ h} & t = 48\text{ h.} \end{array}$$

For CV2 and CV4, the interlayer distances (2.45 and 2.47 nm, respectively), and the calculated number of dye molecules per chemical formula (36 and 38, respectively) are much closed to each other. This suggests that the dye molecules in the interlayer galleries of the two materials arranged themselves in similar modes perpendicularly to the inorganic layers (Fig. 5b).

The calculated chemical formulae of CV3 and CV4 are confirmed by differential thermal analysis (DTA; Fig. 12).

A similarity in the thermal behavior between CV3 and CV4 are observed along all the weight loss intervals. The DTA curves show that there are weight loss between 25 and 150 °C caused by the hydration water (6.61 and 5.44%, respectively), and second peak between 150 and 250 °C corresponds to both, loss of methylammonium and partial decomposition of the surfactant (4.80 and 3.22%, respectively). As a results of the decomposition of the remaining surfactant in CV3 and CV4 (6.05 and 3.19%, respectively), the third weight loss is occurred between 250 and 350 °C.

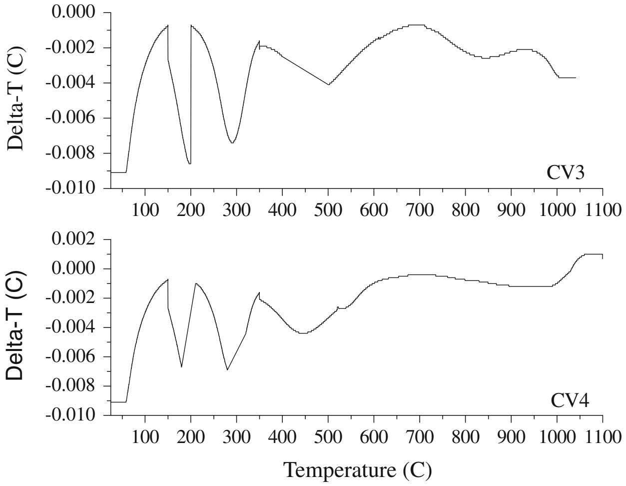

Fig. 12 DTA curves of CV3 and CV4

Even the overlapping between the weight loss intervals of methylammonium and surfactant does not permit the calculation of the exact mole ratio between both of them, the experimental measurement of total weight loss (10.85% and 6.41%, respectively) indicates that it is much closed to the calculated percentage of methylammonium and HY (10.78 and 6.32%, respectively) in the chemical formulae of CV3 and CV4.

As a result of dye decomposition, fourth weight loss takes place between 350 and 650 °C in DTA thermograms of CV3 and CV4. This decomposition corresponds to weight losses of 16.00% and 29.44%, respectively. The later percentages are compatible with the calculated amount of the dye in the formulae of CV3 and CV4 (15.87 and 29.49%, respectively).

The UV–Vis spectra of CV3 and CV4 are recorded in suspension (Fig. 13). By observation, actually, there is no shift for the characteristic band of CV (590 nm) in the spectra of the two materials.

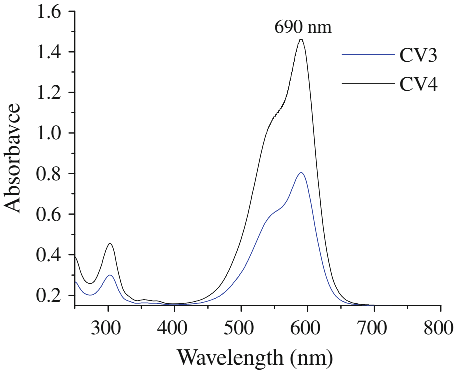

Fig. 13 UV-Vis spectra of CV3 and CV4 (suspension of 8 mg of the solid in 10 mL of water)

As a reasonable clarification for the recent observation, the dye in CV3 and CV4 could be monovalent cation (CV^+) and has approximately the same conjugated system of CV in aqueous solution.

This explanation is compatible with the proposed reactions between CV and γ-ZrPHY. The reaction between CV and γ-ZrPHY is double replacement reaction.

With respect to this reaction, all of the $O_2P(OH)_2$ groups of the inorganic layers are already reacted with methylamine of HY molecules, so no valuable change in the conjugated system of CV is expected.

It is very essential to highlight the following comments, as CV4 has higher absorbance (1.46) than CV3 (0.81), its dye content is higher than that one in CV3, also, with reference to the absorbance values of CV1 (0.66) and CV2 (1.31), the dye contents of the four synthesized materials can be arranged as follows: CV4 > CV2 > CV3 > CV1. This fact seems to be in accordance with the calculated chemical formulae of the four materials.

As Fig. 14 shows the FT-IR spectra of γ-ZrPHY, CV3 and CV4, first, it is clear that the spectrum of γ-ZrPHY is a composites of those of γ-ZrP and the respective alkyl ammonium compounds ($MeNH_3^+$ and HY). Second, the spectra of CV3 and CV4 are composites of those of γ-ZrP, $MeNH_3^+$, HY and the free dye.

γ-ZrPHY shows absorption peaks at 2,928, 2,849, 1,474 and 721 cm^{-1} are belong to the characteristic peaks of HY and $CH_3NH_3^+$. Among of them, two strong peaks at 2,928 and 2,849 cm^{-1} originate from the stretch of $-CH_2-$ and $-CH_3$ of saturated hydrocarbon, respectively. The peak at 721 cm^{-1} results from the vibration of $-(CH_2)_n-$ bond.

In addition, there are two peaks more, one at 1,620 cm^{-1} and another at 3,400 cm^{-1} corresponding to H–O–H confirm the existence of crystalline H_2O in γ-ZrPHY.

It is notable from FT-IR spectra, that the band of γ-ZrPHY at 1,620 and 1,474 cm^{-1} are weakened after intercalation of dye inside the solid matrices (CV3 and CV4). This result could be attributed to the increase in the hydrophobicity of the solid materials after replacing HY and $MeNH_3^+$ cations by the dye cations in γ-ZrPHY, therefore the chemical formulae of CV3 and CV4 have lower HY, $MeNH_3^+$ and water molecules per formula with respect to that of γ-ZrPHY precursor.

Moreover, it is important to mention that the intensity of band at 1,620 cm^{-1} is higher in the FT-IR spectrum of CV4, which means that CV4 has higher dye content than CV3 where this result seems to be in accordance with the calculated chemical formulae of CV3 and CV4.

In conclusion, the chemical formulae of CV1, CV2, CV3 and CV4 have been confirmed by elemental and thermogravimetric analyses, UV–Vis and FT-IR spectrophotometries. Relatively, a time of 48 h is necessary to

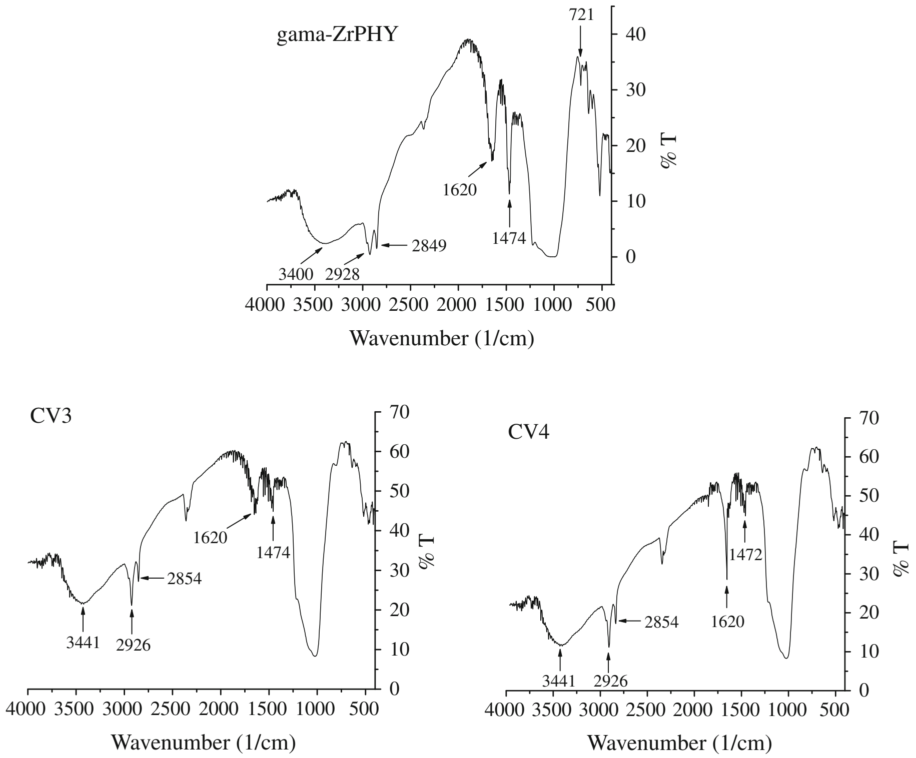

Fig. 14 FT-IR spectra of γ-ZrPHY, CV3 and CV4

Table 1 Comparison of adsorption capacities of various materials for CV

Adsorbent	Ads. cap./mg g^{-1}	*T*/°C	[Ref.]
γ-ZrP	320.20	RT	Present work
γ-ZrPHY	322.48	RT	Present work
Magnetic nanocomposite	111.80	50	[22]
Calcined ball clay	65.28	50	[23]
Uncalcined ball clay	77.52	50	[23]
CTMA-bentonite composite	239.10	45	[24]
BTEA-bentonite composite	222.69	30	[24]
Calcined mixed clay	775.2	50	[25]
Semi-IPN hydrogels	28.6	25	[26]
Tamarind seed powder	14.28	57	[27]
Polyacrylamide-bentonite composite	144.60	30	[28]
Raw kaolin	44.88	26	[26]
Amorphous ZrP (sol–gel method)	277.73	60	[10]
Jute fiber carbon	27.74	32	[29]
Palygorskite	57.94	25	[30]
Raw sepiolite	73.44	36	[31]
Surfactant-modified alumina	60	20 ± 2	[32]
Activated carbon	64.875	40	[33]
Activated carbon (PAAC)	60.38	28	[34]
MCM-22	48.96	30	[35]
Bagasse fly ash	26.23	30	[36]
Unexpanded perlite	3.30	30	[37]
Expanded perlite	1.14	30	[37]
Activated carbon from sewage sludge	68.14	30	[38]
Activated carbon from coconut husk	61.61	30	[38]
α-ZrP	229.03	RT	[9]

obtain purer phases and higher dye uptakes. γ-ZrP and γ-ZrPHY show maximum dye uptake capacities of 18 and 19%, respectively, which is closely related to the estimated value by molecular modeling (ca. 20%). Moreover, HY surfactant assists the huge dye molecules to be intercalated in the interlayer galleries of γ-ZrP in order to obtain a much purer phase of CV4.

Comparison of various adsorbents

The following table summarizes the maximum adsorption capacities observed in the present work and those reported in the literatures for other adsorbents. From the table, it is clear that the uptake capacities of both γ-ZrP and γ-ZrPHY (320.20 and 322.48 mg g^{-1}, respectively) are almost greater that the others except one material (see below Table 1).

Accordingly, the obtained results give practical realistic evidences that γ-ZrP and γ-ZrPHY are worthy efficient materials for the removal of CV dye as they would be used as a competitive alternate for almost all of others included inside the table.

Conclusion

The pristine γ-ZrP and γ-ZrPHY show very high dye uptake (ion-exchange) capacities towards CV (18 and 19%, respectively).With respect to the previous mentioned dye uptake, they are very close to the calculated maximum one (ca. 20%). In addition they are dependent of the interlayer distances of the layered materials and the mode in which CV molecules are arranged inside the interlayer gallery. The highest dye uptake capacities are observed when the dye molecules arrange themselves perpendicularly to the inorganic layers. The pre-intercalation of γ-ZrP with the surfactant molecules facilitates the diffusion process of the dye molecules to be smoothly exchanged inside the interlayer gallery.

The results achieved by the current research reinforce those obtained in our recent one about malachite green [see ref. 11], where in two researches, γ-ZrP and zirconium phosphate/surfactant composite (γ-ZrPHY) reveal that they are extremely efficient in removing both triphenylmethane dyes.

Acknowledgments The authors are grateful to the *Association of Arab Universities* for financial support and to Mr. Kamal Alhendawi for English revision.

References

1. Bangert, R., Aichele, W., Schollmeyer, E., Weimann, B., Herlinger, H.: Melliand Textilber. **58**, 399 (1977)
2. Bumpus, J.A., Brock, B.J.: Appl. Environ. Microbiol. **54**, 1143 (1988)
3. Chen, C.C., Liao, H.J., Cheng, C.Y., Yen, C.Y., Chung, Y.C.: Biotechnol. Lett. **29**, 391 (2007)
4. Alberti, G., Costantino, U.: Intercalation chemistry. In: Whittingham, M.S., Jacobson, A.J. (eds.), Chap. 5, pp. 147–180. Academic Press, New York (1982)
5. Hasegawa, Y., Tomita, I.: Trends Inorg. Chem. **2**, 171 (1991)
6. Feng, Y., He, W., Zhang, X., Jia, X., Zhao, H.: Mater. Lett. **61**, 3258 (2007)
7. Panwar, O.P., Kumar, A., Ameta, R., Ameta, S.C.: Maced. J. Chem. Chem. Eng. **27**, 2–133 (2008)
8. Barhon, Z., Albizane, A., Azzi, M., Saffaj, N., Bennazha, J., Yo Unssi, S.A.: J. App. Sci. Res. **5**(7), 893 (2009)
9. Hoppe, R., Alberti, G., Costantino, U., Dionigi, C., Schulz-Ekloff, G., Vivani, R.: Langmuir **13**, 7252 (1997)
10. Jayswal, A., Chudasama, U.: Indian J. Chem. Technol. **14**, 597 (2007)
11. Alhendawi, H.M.H.: J. Mater. Chem. **21**, 7748 (2011)
12. Shi, S., Zong, R., Liu, Y., Wang, Y., Zhou, J.: Key Eng. Mater. **336–338**, 2589 (2007)
13. Alberti, G., Bernasconi, M.G., Casciola, M.: React. Polym. **11**, 245 (1989)
14. Clearfield, A., Costantino, U.: Comprehensive supramolecular chemistry. In: Alberti, G., Bein, T. (eds.). vol. 7, Chap. 4, pp. 107–150. Pergamon, New York (1996)
15. Conant, J.B., Werner, T.H.: J. Am. Chem. Soc. **52**, 4436 (1930)
16. Rajeh, A.O., Szirtes, L.: J. Radioanal. Nucl. Chem. **241**(1), 83 (1999)
17. Van Damme, H., Crespin, M., Obrecht, F., Cruz, M.I., Eripiat, J.J.: J. Colloid Interface Sci. **66**, 43 (1978)
18. Tomita, I., Takeo, C.: J. Incl. Phenom. Mol. Recognit. Chem. **9**, 315 (1990)
19. Brunet, E., de la Mata, M.J., Juanes, O., Alhendawi, H.M.H., Cerro, C., Rodríguez-Ubis, J.C.: Tetrahedron Asymmetr. **17**(3), 347 (2006)
20. Brunet, E.: Chirality **14**, 135 (2002)
21. Alberti, G., Cardini-Galli, P., Costantino, U., Torracca, E.: J. Inorg. Nucl. Chem. **29**, 571 (1967)
22. Singh, K.P., Gupta, S., Singh, A.K., Sinha, S.: J. Hazard. Mater. **186**(2–3), 28–1462 (2011)
23. Monash, P., R.N., Pugazhenthi, G.: Clean Technol. Environ. Policy. **13**, 141 (2011)
24. Jian-min, R., Si-wei, W., Wei, J.: World Acad. Sci. Eng. Technol. **65**, 790 (2010)
25. Monash, P., Pugazhenthi, G.: Sep. Sci. Technol. **45**(1), 94 (2010)
26. Li, S.: Bioresour. Technol. **101**(7), 2197 (2010)
27. Patel, H., Vashi, R.T.: E-J. Chem. **7**(3), 975 (2010)
28. Anirudhan, T.S., Suchithra, P.S., Radhakrishnan, P.G.: Appl. Clay Sci. **43**, 336 (2009)
29. Porkodi, K., Vasanth kumar, K.: J. Hazard. Mater. **143**, 311 (2007)
30. Al-Futaisi, A., Jamrah, A., Al-Hanai, R.: Desalination **214**, 327 (2007)
31. Eren, E., Afsin, B.: Dyes Pigments **73**, 162 (2007)
32. Adak, A., Pal, A.: J. Environ. Sci. Health Part A **41**(10), 2283 (2006)
33. Kaustubha Mohanty, Thammu Naidu, J., Meikap, B.C., Biswas, M.N.: Ind. Eng. Chem. Res. **45**(14), 5165 (2006)
34. Senthilkumaar, S., Kalaamani, P., Subburaam, C.V.: J. Hazard. Mater. **136**, 800 (2006)
35. Wang, S., Li, H., Xu, L.: J. Colloid Interface Sci. **295**, 71 (2006)
36. Mall, I.D., Srivastava, V.C., Agarwal, N.K.: Dyes Pigments **69**, 210 (2006)
37. Dogan, M., Alkan, M.: J. Colloid Interface Sci. **267**, 32 (2003)
38. Graham, N., Chen, X.G., Jayaseelan, S.: Water Sci. Technol. **43**, 245 (2001)